

Respiratory Induced Resonance Offset Correction for PRFS Temperature Maps

A. V. Shmatukha¹, C. J. Bakker²

¹Image Sciences Institute, University Medical Center Utrecht, Utrecht, Netherlands, ²Radiology Department, University Medical Center Utrecht, Utrecht, Netherlands

INTRODUCTION: The Proton Resonance Frequency Shift (PRFS) method of MRI temperature mapping cannot discriminate between the phase accumulated by protons due to temperature changes and the phase accumulated by the same protons due to local magnetic field changes (1). Respiration disturbs the magnetic field in anatomies proximal to the lungs (2) and even in the head (3) – the Respiratory Induced Resonance Offset (RIRO) effect. The higher the temporal and spatial resolution of a temperature mapping process is, the less the RIRO-caused phase disturbances are averaged over the breathing cycle and anatomy volume, which leads to bigger errors in the resulting temperature estimation. An applicable correction method proposed earlier (4) demands access to the raw k-space data stored on a scanner and sophisticated post-processing of this data. Our method uses only reconstructed images, no k-space operations and a minimum of calculations using a small ROI. It is based on the Adaptive Subtraction method (5) and uses two types of baseline phase maps – one for temperature and another one for RIRO-induced field disturbances. Our method is shown to improve the accuracy and stability of PRFS temperature maps in the presence of RIRO and motion in phantom experiments.

THEORY: Images of any type can be identified as acquired at the identical instants of the respiratory cycle with the help of the non-similarity coefficients (NSC's):

$$\lambda^m = \frac{\sum_{i=1}^{N_i} \sum_{j=1}^{N_j} (\xi_{ij}^m - \xi_{ij}^1)^2}{\sum_{i=1}^{N_i} \sum_{j=1}^{N_j} (\xi_{ij}^1)^2} \quad [1]$$

where λ^m denotes the NSC calculated on the image number “m”; ξ_{ij}^m denotes the intensity value of the (i-th; j-th) pixel in a ROI

chosen on the image number “m”; N_i and N_j denote the corresponding dimensions of the ROI in pixels. The NSC's express how the RIRO effects vary with time in comparison to the very first pre-treatment image. The NSC's take similar values for identical lung volumes and surrounding anatomy positions. As the sensitivity of the NSC's can be handicapped by phase wrap-arounds and intra-voxel dephasing, a dual-echo acquisition is used. The images from the shorter TE are used for calculating the NSC's, while the images from the longer TE are used to calculate the temperature maps themselves. As the MRI parameters of the treated tissue change with temperature, the NSC's have to be calculated on a ROI chosen far enough from the thermal treatment site to stay under constant temperature. Suppose, there are two pre-treatment complex images D_a and D_b as well as two successive intra-treatment complex images D_γ and D_δ acquired at the corresponding identical instants of the respiratory cycle. The temperature map can be calculated in two ways: $T_{\delta,\gamma}^A = (D_\delta D_\gamma^*) \times (D_\gamma D_a^*)^*$ or $T_{\delta,\gamma}^B = (D_\delta D_\gamma^*) \times (D_b D_a^*)^*$ [2]. While both ways lead to the same result and have the same SNR, they differ by temperature and RIRO dynamic ranges that they can cover without phase wrap-arounds. Our method's SNR is lower by a factor of $\sqrt{2}$ as compared to the traditional PRFS.

METHODS: Image processing was performed using IDL V.6.1. MRI was performed on a 1.5-T Intera-NT (Philips MS) with the help of a surface coil. Porcine muscle specimens were imaged using 2D FGRE EPI. In all experiments, fat suppression was executed by using a binominal saturation pulse and shimming was applied. No hardware drift compensation was applied to the temperature maps. In phantom and heating experiments, a cylinder made from a non-ferromagnetic alloy was moved manually between image acquisitions to simulate RIRO (Fig. 1). In heating experiment, one of the specimens was heated using a laser (Diomed Ltd., Cambridge, UK) and its temperature was sampled at 3 points using a fluoroptic thermometer (Luxtron Corp., Santa Clara, CA, USA). One 5mm- thick slice was acquired in 3.9 sec. with in-plane spatial resolution of 1.37x1.37 mm using TR/TE1/TE2/FA/ETL = 75 ms/9.20 ms/20.70 ms/45° /3. In motion experiments, one of the meat specimens was moved manually 7 inch away from its initial position and back two times in steps of 1 inch. The specimen temperature (which stayed constant) was calculated from the last 24 images using the first 8 ones as baseline. One 5mm- thick slice was acquired in 8.5 sec. with in-plane spatial resolution of 1.76x1.76 mm using TR/TE1/TE2/FA/ETL = 100 ms/9.20 ms/20.70ms/27° /3.

RESULTS: The NSC's calculated on the phase images acquired during the cylinder movement experiment (Fig. 2) stayed well defined in spite of magnetic field disturbances reaching 2.5 ppm. Periodical movements of one of the meat specimens induced periodical magnetic field disturbances, so PRFS reported an artifact temperature evolution (Fig. 3). The application of our method eliminated the temperature error in the moving specimen. The temperature calculated using the PRFS method in the laser heating experiment oscillated synchronously with metal cylinder repositioning because it contained a large contribution from the resulting field disturbances (Fig. 4). While the bias of these oscillations changed during the heating and cooling periods, the calculated temperature values were wrong. The temperatures calculated by our method were free of phase contributions due to field disturbances and in good agreement to the readings of the fluoroptic thermometer because the pre-heating images were used as RIRO-baselines.

CONCLUSIONS: In contrary to the method proposed by K. Vigen et al. (4), our method is very easy to implement on a regular clinical scanner and to use in everyday clinical practice. Our method demands neither accessing the raw k-space data nor post-processing it. The acquisition of the baseline pre-treatment images can be performed during 2-3 respiratory cycles with an image acquisition time about 1 sec. without any operator feed-back or decision making. The application of our method substantially reduces errors in PRFS temperature maps due to RIRO and motion. The method's clinical usage will demand developing a proper real-time image transfer and post-processing software as well as a safety control mechanism.

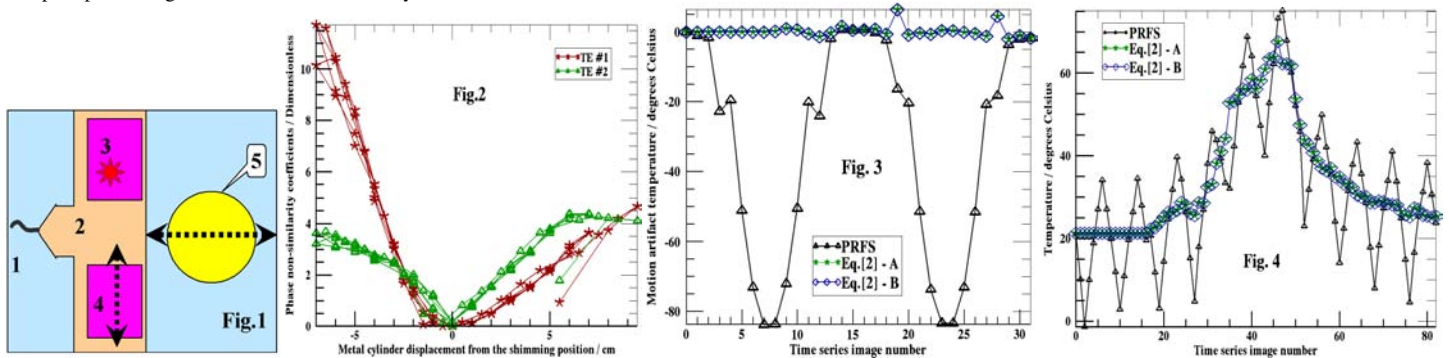


Fig.1: Experimental set-up: 1- scanner bed; 2- surface coil; 3- "thermally treated" specimen; 4- periodically moving specimen; 5- periodically moving metal cylinder. **Fig.2:** The phase NSC's calculated in the metal cylinder movement experiment as a function of the cylinder's displacement from its initial (shimming) position. **Fig.3:** Artifact temperature evolution in a moving meat specimen (3x3 px averaged). The initial specimen temperature was deliberately assigned to be zero. **Fig.4:** The averaged temperature of a 3x3 px ROI located nearby the optical fiber tip during the laser heating experiment.

REFERENCES: 1. D. Germain et al., MAGMA 13, 47-59 (2001). 2. P.J. Bolan et al., MRM 52, 1239-1245 (2004). 3. J.P. Marques et al., Concepts Magn. Reson. 25B, 65-78 (2005). 4. K.K. Vigen et al., MRM 50, 1003-1010 (2003). 5. C.J.G. Bakker et al., JMRI 20, 470-474 (2004).